Journal of Materials Chemistry C

Materials for optical, magnetic and electronic devices

Accepted Manuscript

Journal of
Materials Chemistry C

Materials for optical, magnetic and electronic devices

rsc.li/materials-c

Volume 6
Number 5
7 February 2018
Pages 911-1266

ISSN 2050-7526

ROYAL SOCIETY
OF CHEMISTRY

PAPER
Nosang V. Myung, Yong-Ho Choa *et al.*
A noble gas sensor platform: linear dense assemblies of
single-walled carbon nanotubes (LACNTs) in a multi-layered
ceramic/metal electrode system (MLES)

ROYAL SOCIETY
OF CHEMISTRY

rsc.li/materials-c

Journal of Materials Chemistry C

COMMUNICATION

Anti-Oxidative Passivation and Electrochemical Activation of Black Phosphorus *via* Covalent Functionalization and Its Nonvolatile Memory Application

Weilin Chen,[a,b] Shuang Gao,*[a] Zhuolin Xie,[a,b] Ying Lu,[a,b] Guodong Gong,[a,b] Gang Liu,*[c] Jie Shang,[a] Chuang Yao,[d] and Run-Wei Li*[a]

As a novel layered semiconductor that can bridge the energy band and carrier mobility gaps between graphene and transition metal dichalcogenides, black phosphorus (BP) has broad prospects in optoelectronics and nanoelectronics. Nevertheless, the contradiction between excellent semiconducting properties and easy oxidation under ambient conditions is difficult to reconcile. Herein, the first demonstration of protection and regulation of BP by introducing redox-active moieties of triphenylamine (TPA) is reported. The prepared BP nanosheets grafted covalently with TPA molecules (BPNSs-TPA) exhibit excellent anti-oxidative capability and electrochemical activity. As a proof of concept, the BPNSs-TPA are successfully used to construct a nonvolatile redox-based resistive switching memory, showing good working stability and durability. Meanwhile, potentiation and depression characteristics of a biological synapse are well emulated within the memory cell. These demonstrations could provide a powerful way to protect and functionalize BP through organic small molecules, which is of great significance for the application of BP in memory and neuromorphic devices.

As a novel layered semiconducting material, black phosphorus (BP) has attracted widespread attention since the first exfoliation in 2014.[1] With the superior properties of layer-dependent direct bandgap,[2] high carrier mobility,[3] and strong in-plane anisotropy,[4] BP has exhibited promising applications in microelectronics,[5] optoelectronics,[6] biomedicine,[7] energy conversion,[8] and so on. Noting that, within a single BP layer, each P atom forms three covalent bonds with neighboring P atoms through sp^3 hybridization, leaving a lone pair of

electrons on the forth orbital.[9] As such, few-layer BP tends to degrade fast (normally within several hours to a few days) in chemical structure and electronic properties *via* oxidation under ambient conditions, hindering severely its practical applications.[10]

To protect BP from being oxidized, both physical and chemical methods have been recently proposed.[11] Physical methods refer to the encapsulation of BP with a capping layer, such as Al_2O_3 and hBN.[12,13] Despite the high effectiveness to obtain air-stable BP, physical methods are less satisfactory for scalable applications in terms of high cost, complex preparation process, etc. Excitingly, these drawbacks can be well eliminated by chemical passivation in the form of covalent modification[11] or surface coordination.[14] In particular, covalent modification of BP *via* aryl diazonium salts to form C-P bonds can greatly deplete the lone-pair electrons and thus fundamentally solve the easy oxidation issue. Also, thanks to the strong interaction between the grafting organic molecules and BP, improved properties or expanded functions can sometimes be expected after modification.

The covalent modification of BP *via* aryl diazonium salts was put forward by Hersam et al.[15] in 2016. They observed both high chemical stability and improved semiconducting properties (specifically, hole mobility) in exfoliated BP nanosheets (BPNSs) after being modified by 4-nitrobenzene-diazonium tetrafluoroborate. Inspired by that work, Chen et al.[16] recently pioneered the synthesis of polymer-grafted BPNSs with the help of aryl diazonium salt-modified BPNSs as the key template materials. It is surprising that, besides high chemical stability, good dispersibility in organic solvents and even unexpected electrical activity were demonstrated in the obtained polymer-grafted BPNSs. As such, the modified BPNSs were further introduced for application as the spin-coated active layer of resistive switching memory that is acknowledged as a highly promising candidate for next-generation nonvolatile data storage devices.[17,18] The working mechanism was attributed to the electrical activity of the modified BPNSs, that is, electric field-induced reversible charge transfer between the grafting polymer molecules and BPNSs.

[a.] CAS Key Laboratory of Magnetic Materials and Devices, and Zhejiang Province Key Laboratory of Magnetic Materials and Application Technology, Ningbo Institute of Materials Technology and Engineering, Chinese Academy of Sciences, Ningbo 315201, China. Email: gaoshuang@nimte.ac.cn, runweili@nimte.ac.cn
[b.] College of Materials Sciences and Opto-Electronic Technology, University of Chinese Academy of Sciences, Beijing 100049, China
[c.] School of Electronic Information and Electrical Engineering, Shanghai Jiao Tong University, Shanghai 200240, China. Email: gang.liu@sjtu.edu.cn
[d.] Key Laboratory of Extraordinary Bond Engineering and Advance Materials Technology (EBEAM) of Chongqing, School of Materials Science and Engineering, Yangtze Normal University, Chongqing 408100, China
†Electronic Supplementary Information (ESI) available: [details of any supplementary information available should be included here]. See DOI: 10.1039/x0xx00000x

Despite these huge progresses, the grafting process of polymer molecules onto BPNSs is somewhat complicated, needing two or more key reaction steps. Also, the charge-based working mechanism could make related memory devices incompatible between a long data retention time and a fast operation speed.[19] Both points are certainly unfavorable for the practical applications of polymer-grafted BPNSs in nonvolatile memory devices.

Herein, we report for the first time the realization of anti-oxidative passivation and electrochemical activation of BPNSs *via* a facile one-step covalent modification process using diazonium tetrafluoroborate of triphenylamine (DTPA). The successful grafting of TPA molecules onto BPNSs *via* covalent C-P bonds has not only been well supported by theoretical calculations but also been definitely confirmed by various spectroscopic analyses. Compared with the as-exfoliated BPNSs, the BPNSs grafted with TPA molecules (abbreviated as BPNSs-TPA) are found to exhibit a remarkable improvement of ~5 times in anti-oxidative capability. More importantly, distinct electrochemical activity and good dispersibility in organic solvents are demonstrated in BPNSs-TPA at the same time. With these superior characteristics, the BPNSs-TPA have been further used as the key component to construct an air-stable redox-based analog resistive switching memory, showing promising applications not only as a bistable electronic device for data storage but also as an artificial synapse for neuromorphic computing.
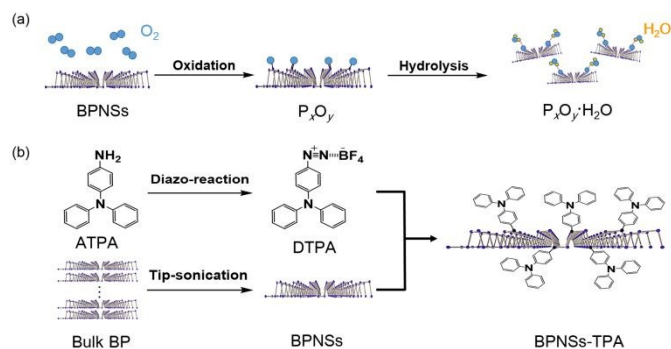
Figure 1. Degradation process of BPNSs and synthesis procedure of BPNSs-TPA. a) Schematic illustration of the degradation process of BPNSs in ambient conditions. b) Schematic illustration of the synthesis procedure of DTPA, the delamination procedure of BPNSs, and the reaction process of BPNSs and DTPA to form BPNSs-TPA.

BPNSs are known to degrade easily in atmosphere.[20] **Figure 1a** shows the typical ambient degradation process of BPNSs. In brief, they are firstly oxidized to P_xO_y and then decompose completely with the participation of H_2O molecules.[14] Such process is extremely disadvantageous for the practical use of BPNSs in electronic devices. To resolve this issue, we herein report a one-step and scalable preparation process for small organic molecule-modified BPNSs, through which the BPNSs could simultaneously have excellent chemical stability and electrochemical activity, as shown in **Figure 1b**. The successful synthesis of DTPA *via* diazotization was verified by Fourier

transform infrared (FTIR) analysis and ^{1}H nuclear magnetic resonance (NMR) spectrum (**Figure S1 and S2**). As for BPNSs, they were exfoliated from bulk BP *via* tip ultrasonication, exhibiting an average height and size of ~7 nm and ~148 nm, respectively (**Figure S3** and **S4**). To obtain the final product of BPNSs-TPA, the synthesized DTPA and exfoliated BPNSs were dispersed in acetonitrile and stirred vigorously in an argon-filled condition for 5 hours, followed by several centrifugation and washing processes to remove raw materials. More details can be found in the Experimental Section in ESI.
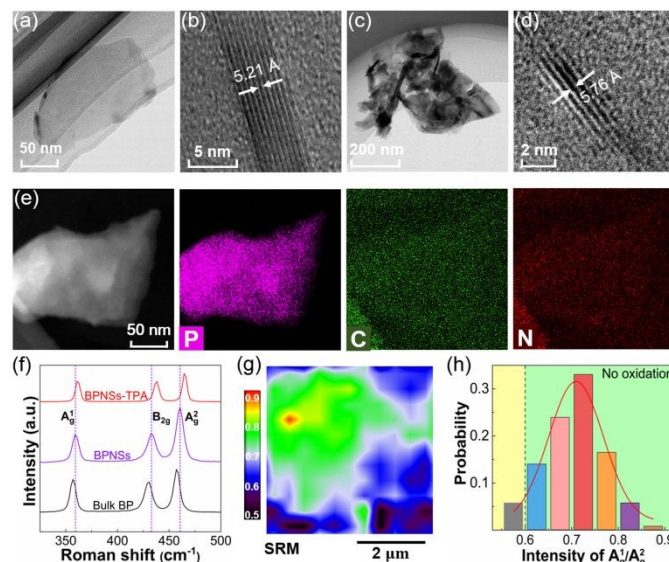

Figure 2. Characterization of BPNSs and BPNSs-TPA. a-b) TEM morphology and lattice images of BPNSs. c-d) TEM morphology and lattice images of BPNSs-TPA. e) TEM image and EDS maps of BPNSs-TPA. f) Raman spectra of bulk BP, BPNSs and BPNSs-TPA. g) Scanning Raman microscopy mapping of BPNSs-TPA based on the A^1_g/A^2_g intensity ratio. h) Statistical histogram of the A^1_g/A^2_g intensity ratio in g).

A series of methods have been used to characterize the synthesized BPNSs-TPA as well as the exfoliated BPNSs. **Figure 2a** and **2b** show the transmission electron microscopy (TEM) morphology and lattice images of a typical BPNS, respectively. The uniform surface morphology and near-ideal interlayer distance of 5.21 Å both confirm a high crystalline quality of the exfoliated BPNSs.[21] In sharp contrast, some black agglomerates are clearly observed on BPNSs-TPA (**Figure 2c**), which is understandable and can be ascribed to the bonding of organic TPA molecules onto the surface of BPNSs. Also, a clear interlayer distance expansion of ~11% (from 5.21 Å to 5.76 Å) is revealed in BPNSs-TPA (**Figure 2d**), indicating the possible intercalation of some TPA molecules with small weight into the interlayer spaces of BPNSs. It is noted that the intercalation of exotic molecules into BPNSs could help to archive a better passivation effect.[22] Moreover, through energy-dispersive X-ray spectroscopy (EDS) analysis, the C and N elements are found to exist definitely in BPNSs-TPA (**Figure 2c**) but absent almost completely in BPNSs (**Figure S5**), confirming again the successful bonding of TPA molecules to BPNSs during the modification process.

Raman spectrum measurements were performed to further evaluate the effect of modification process on the lattice structure of BPNSs. **Figure 2f** shows the comparison of Raman spectra between BPNSs and BPNSs-TPA, in which the Raman spectrum of bulk BP is also provided as a reference. The observed three prominent peaks from left to right in each spectrum can be ascribed to the out-of-plane phonon mode (A^1_g), the in-plane mode along zigzag direction (B_{2g}), and the in-plane mode along armchair direction (A^2_g), respectively.[23] One can see that, compared with bulk BP, blue shifts of these characteristic Raman peaks occur clearly in BPNSs and more notably in BPNSs-TPA. The former is considered to be caused by size reduction after exfoliation, whereas the latter indicates an additional intermolecular interaction between BPNSs and TPA molecules after modification. These findings are in good agreement with previous reports concerning the covalent modification of BPNSs,[16] demonstrating further the successful bonding of TPA molecules to BPNSs during the modification process. In addition, scanning Raman analysis was conducted to reveal the oxidation degree of BPNSs immediately after the modification process. As shown in **Figure 2g** and **2h**, about 95 percent of the measured points have a A^1_g/A^2_g peak ratio of greater than 0.6, leading to an average value of ~0.72. Representative Raman spectra of different A^1_g/A^2_g peak ratio regions can be found in **Figure S6**. It is noted that a A^1_g/A^2_g peak ratio of no less than 0.6 demonstrates the avoidance of BP materials from being oxidized.[24] As such, it is reasonable to conclude that our modification process is very mild and has little oxidation effect on BPNSs.
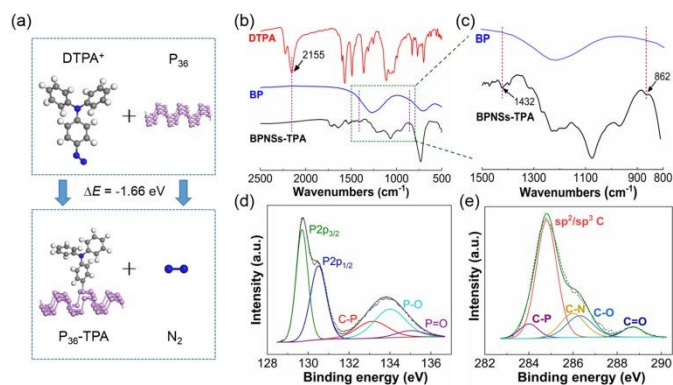
Figure 3. Theoretical calculations and spectroscopic analyses on BPNSs-TPA. a) DFT-calculated reaction process and energy of grafting DTPA molecules onto BPNSs. b-c) FTIR spectra of the samples. d-e) High-resolution P2p and C1s XPS spectra of BPNSs-TPA.

To provide solid evidences for the expected formation of covalent bonding between BPNSs and TPA molecules during the modification process, both theoretical calculations and spectroscopic analyses have been made. **Figure 3a** shows the optimized structure of BPNSs-TPA *via* density functional theory (DFT) calculations, where a unit cell consists of 36 P atoms and one DTPA molecule. The reaction driving energy per unit cell was calculated to be −1.66 eV based on $\Delta E = E(P_{36}\text{-TPA}^+) + E(N_2) − E(P_{36}) − E(DTPA^+)$, where $E(P_{36}\text{-TPA}^+)$, $E(N_2)$, $E(P_{36})$, and

$E(DTPA^+)$ represent the formation energies of $P_{36}\text{-TPA}^+$, N_2, P_{36}, and $DTPA^+$ molecules, respectively. Such a value demonstrates that the formation of covalent C-P bonds in BPNSs-TPA is highly favourable from the viewpoint of thermodynamics. The comparison in FTIR spectra between BPNSs and BPNSs-TPA is provided in **Figure 3b** and **3c**. One can see that, compared to BPNSs, there are two newly appeared peaks at ~1432 cm^{-1} and ~862 cm^{-1} in BPNSs-TPA, which are distinctive characteristics for the C-P bond.[25] Also, the characteristic vibrational peak of diazo group (-N_2^+) at ~2155 cm^{-1} disappears completely after modification, indicating no residual DTPA molecules in BPNSs-TPA. On the other hand, X-ray photoelectron spectroscopy (XPS) analysis of BPNSs-TPA reveals clear contributions from C-P bond in both P 2p spectrum at ~133.4 eV and C 1s spectrum at ~284.2 eV, as shown in **Figure 3d** and **3e**, respectively.[16] These results together can demonstrate definitely that, in the synthesized BPNSs-TPA, the interaction between TPA molecules and BPNSs is indeed through the expected C-P covalent bond.
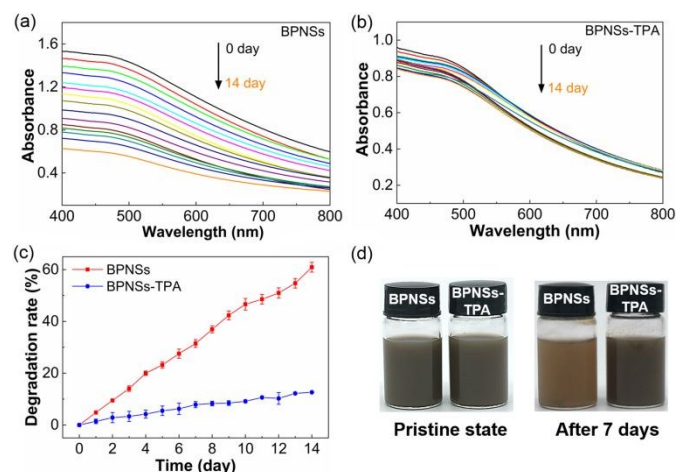
Figure 4. Anti-oxidative capability and dispersibility of BPNSs and BPNSs-TPA. UV-Vis absorption spectra of a) BPNSs and b) BPNSs-TPA dispersed in water after exposure to air for 14 consecutive days. c) Degradation rates of BPNSs and BPNSs-TPA with 14 consecutive days. d) Digital pictures of BPNSs and BPNSs-TPA dispersed in ethanol immediately after sonication and after 7 days.

With successful covalent modification, anti-oxidative performance of the synthesized BPNSs-TPA was firstly evaluated through time-dependent ultraviolet-visible (UV-Vis) absorption spectroscopy. For such analysis, the BPNSs-TPA were dispersed in water and stored under ambient conditions for two weeks. Similar analysis was also conducted on BPNSs for comparison. According to the Lambert-Beer law, the optical absorbance A of a liquid solution can be expressed by $A = K \cdot b \cdot c$, where K is the molar absorption coefficient, b is the sample thickness, and c is the sample concentration. As such, the oxidation-caused degradation of BP in solution can be well reflected through monitoring the time-dependent change in absorbance at a specific wavelength. **Figure 4a** and **4b** show the time-dependent absorbance spectra of BPNSs and BPNSs-TPA, respectively. One can readily see that, within two weeks,

COMMUNICATION

Journal Name

the absorption capability of BPNSs decreases significantly over time, whereas that of BPNSs-TPA exhibits only a slight decrease. Further, the absorption data at 400, 450, 500 and 550 nm were normalized and statistically analysed to quantitatively reflect the degradation processes of BPNSs and BPNSs-TPA, as shown in **Figure 4c**. A high degradation ratio of ~61% is calculated for BPNSs after exposure in atmosphere for two weeks, which is in good agreement with the easy oxidation property of BP.[26] In sharp contrast, only a small degradation ratio of ~13% is obtained for BPNSs-TPA, indicating a remarkable improvement of ~5 times in anti-oxidative capability of BPNSs after covalent modification by TPA. More importantly, the BPNSs-TPA is found to have an almost top-ranked stability when compared with its counterparts in previous studies (**Figure S7**),[14,27-32] demonstrating further the high effectiveness of our modification process for BP passivation. In addition, good dispersibility of BP in organic solvents is necessary for practical applications in devices that are fabricated *via* simple and cost-effective solution methods like spin-coating. As shown in **Figure 4d**, the BPNSs-TPA dispersed in ethanol has almost no sedimentation after 1 week, while the BPNSs exhibit obvious sedimentation after the same time period, accompanied by a much lighter supernatant. This suggests that our modification process can significantly improve the dispersibility of BP in organic solvents at the same time, which is very advantageous for fabricating related devices.[33]
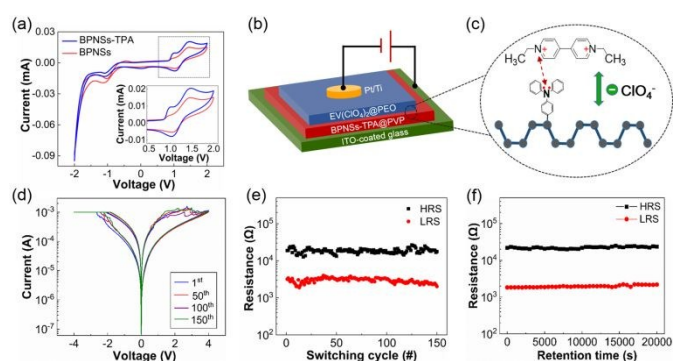
Figure 5. Schematic illustration and characterization of the EV(ClO$_4$)$_2$/BPNSs-TPA-based resistive switching memory. a) CV plots of BPNSs-TPA and BPNSs. The inset shows the enlarged view of the CV plots between 0.5 V and 2 V. b) Schematic device structure of the resistive switching memory. c) Schematic working mechanism of the memory device. d-f) Consecutive resistive switching loops, switching endurance and retention property of the memory device.

Besides high anti-oxidative capability and dispersibility, superior electrochemical activity has also been confirmed in the BPNSs-TPA, as shown in **Figure 5a**. The cyclic voltammetry (CV) curves were obtained by coating the samples on a Pt disk electrode and then placing in a 0.1 M acetonitrile solution of Tetrabutylammonium hexafluorophosphate, with Ag/AgCl as the reference electrode and a Pt wire as the counter electrode. The higher oxidation peaks and larger hysteresis area of the CV loop for BPNSs-TPA demonstrates definitely a highly improved

electrochemical activity when compared to BPNSs. Meanwhile, the onset oxidation potential of BPNSs-TPA (0.88 V) is slightly larger than that for BPNSs (0.83 V) (**Figure S8**), which accords well with the verified higher anti-oxidative capability in BPNSs-TPA. Noting that, the superior electrochemical activity of BPNSs-TPA is highly desired for many applications like nonvolatile memory,[34] energy storage,[35] gas sensor,[36] and biosensor.[37] As a proof of concept, a nonvolatile resistive switching device based on the redox system of BPNSs-TPA and ethyl viologen diperchlorate (EV(ClO$_4$)$_2$) was constructed, as shown in **Figure 5b**. Herein, the EV(ClO$_4$)$_2$ was selected as it has an excellent radical-rich feature and can also provide movable counter ClO$_4^-$ ions for redox system stabilization.[38] Moreover, the polyvinylpyrrolidone (PVP) and polyethylene oxide (PEO) were adopted mainly as the host material for each layer and did not participate in the redox reaction. Within such system, a continuous regulation in the transport property of BPNSs-TPA could be expected through the reversible redox reaction between TPA with EV(ClO$_4$)$_2$, accompanied by the reversible exchange of ClO$_4^-$ ions between the two layers to stabilize the whole system (**Figure 5c**). With indium-tin oxide (ITO) and Pt/Ti as electrodes, the device indeed exhibited a highly stable bipolar resistive switching behavior with good switching endurance of >150 cycles and stable retention of resistance states for >20000 s (**Figure 5d–5f**), thus highly promising for future nonvolatile memory applications. The transition from high resistance state (HRS) to low resistance state (LRS) under negative electric field is attributed to the remove of lone-pair electrons from the N atoms in BPNSs-TPA, leaving themselves in an oxidized, high-conducting state with additional impurity energy levels in the band gap. In the meantime, the cations of EV(ClO$_4$)$_2$ are reduced as the counter electrode reaction, and some ClO$_4^-$ ions from EV(ClO$_4$)$_2$ are driven by the external electric field to move downwards to make the whole system electrically neutral and stable. Subsequently, a positive electric filed will cause the reduction of already positively-charged BPNSs-TPA and backward movement of ClO$_4^-$ ions into EV(ClO$_4$)$_2$, thus switching the device from LRS back into HRS. It is noted that the relatively small switching ratio of ~10 could be further improved through various means in future, such as optimizing the concentration and thickness of the BPNSs-TPA@PVP layer and reducing the memory cell area. Besides nonvolatile memory applications, the gradual resistance change characteristic enables the device to well emulate the potentiation and depression processes of a biological synapse (**Figure S9** and **S10**), thereby being also a potential artificial synapse for future neuromorphic computing applications. Moreover, a control experiment was conducted based on the same device structure by only replacing the BPNSs-TPA by BPNSs (**Figure S11**). Not surprisingly, a very unstable resistive switching behaviour with poor retention of only 2000 s was observed in the control sample. This can definitely demonstrate the decisive role of electrochemical activity of BPNSs-TPA for the resistive switching device stability.

Conclusions

In summary, we report for the first time the successful covalent functionalization of BPNSs *via* small organic molecules of TPA. The covalently bonded TPA molecules can not only effectively protect BPNSs from oxidation but also endow them with a superior electrochemical activity. Meanwhile, the concomitant good dispersibility in organic solvents makes the synthesized BPNSs-TPA feasible to be used in various devices *via* simple and cost-effective solution methods like spin-coating. As a proof-of-concept demonstration, the spin-coated BPNSs-TPA-based memory device can exhibit a highly stable bipolar resistive switching behavior under ambient conditions, with good endurance of >150 cycles and stable retention of >20000 s. Also, potentiation and depression processes of a biological synapse have been well emulated based on such device. These findings could provide a simple yet effective method to functionalize BPNSs for future wide applications in nanoelectronics, optoelectronics, biomedicine, and so on.

Conflicts of interest

The authors declare no competing financial interest.

Acknowledgements

Notes and references

1 L. Li, Y. Yu, G. J. Ye, Q. Ge, X. Ou, H. Wu, D. Feng, X. H. Chen, Y. Zhang, *Nat. Nanotechnol.*, 2014, **9**, 372-377.
2 Y. Akahama, S. Endo, S.-i. Narita, *J. Phys. Soc. Jpn.*, 1983, **52**, 2148-2155.
3 J. Qiao, X. Kong, Z.-X. Hu, F. Yang, W. Ji, *Nat. Commun.*, 2014, **5**, 4475.
4 F. Xia, H. Wang, Y. Jia, *Nat. Commun.*, 2014, **5**, 4458.
5 W. C. Tan, L. Wang, X. Feng, L. Chen, L. Huang, X. Huang, K.-W. Ang, *Adv. Electron. Mater.*, 2019, **5**, 180666.
6 Y. Yi, Z. Sun, J. Li, P. K. Chu, X.-F. Yu, *Small Methods*, 2019, **3**, 1900165.
7 X. Ge, Z. Xia, S. Guo, *Adv. Funct. Mater.*, 2019, **29**, 1900318.
8 J. Pang, A. Bachmatiuk, Y. Yin, B. Trzebicka, L. Zhao, L. Fu, R. G. Mendes, T. Gemming, Z. Liu, M. H. Rummeli, *Adv. Energy Mater.*, 2018, **8**, 1702093.
9 V. V. Korolkov, I. G. Timokhin, R. Haubrichs, E. F. Smith, L. Yang, S. Yang, N. R. Champness, M. Schröder, P. H. Beton, *Nat. Commun.*, 2017, **8**, 1385.
10 M. Batmunkh, M. Bat-Erdene, J. G. Shapter, *Adv. Mater.*, 2016, **28**, 8586-8617.
11 Y. Abate, D. Akinwande, S. Gamage, H. Wang, M. Snure, N. Poudel, S. B. Cronin, *Adv. Mater.*, 2018, **30**, 1704749.
12 J. Pei, X. Gai, J. Yang, X. Wang, Z. Yu, D.-Y. Choi, B. Luther-Davies, Y. Lu, *Nat. Commun.*, 2016, **7**, 10450.
13 S. Gamage, A. Fali, N. Aghamiri, L. Yang, P. D. Ye, Y. Abate, *Nanotechnology*, 2017, **28**, 265201.
14 Y. Zhao, H. Wang, H. Huang, Q. Xiao, Y. Xu, Z. Guo, H. Xie, J. Shao, Z. Sun, W. Han, X.-F. Yu, P. Li, P. K. Chu, *Angew. Chem. Int. Ed.*, 2016, **55**, 5003-5007.
15 C. R. Ryder, J. D. Wood, S. A. Wells, Y. Yang, D. Jariwala, T. J. Marks, G. C. Schatz, M. C. Hersam, *Nat. Chem.*, 2016, **8**, 597-602.
16 Y. Cao, X. Tian, J. Gu, B. Liu, B. Zhang, S. Song, F. Fan, Y. Chen, *Angew. Chem. Int. Ed.*, 2018, **57**, 4543-4548.
17 S. Gao, X. Yi, J. Shang, G. Liu, R.-W. Li, *Chem. Soc. Rev.*, 2019, **48**, 1531-1565.
18 F. Pan, S. Gao, C. Chen, C. Song, F. Zeng, *Mater. Sci. Eng. R.*, 2014, **83**, 1-59.
19 H. Schroeder, V. V. Zhirnov, R. K. Cavin, R. Waser, *J. Appl. Phys.*, 2010, **107**, 054517.
20 Q. Zhou, Q. Chen, Y. Tong, J. Wang, *Angew. Chem. Int. Ed.*, 2016, **128**, 11609-11613.
21 H. Xiao, Z.-S. Wu, L. Chen, F. Zhou, S. Zheng, W. Ren, H.-M. Cheng, X. Bao, *ACS Nano*, 2017, **11**, 7284-7292.
22 S. J. R. Tan, I. Abdelwahab, L. Chu, S. M. Poh, Y. Liu, J. Lu, W. Chen, K. P. Loh, *Adv. Mater.* 2018, **30**, 1704619.
23 S. Qiu, S. Zhou, X. Zhou, T. Zhang, C. Wang, R. K. K. Yuen, W. Hu, Y. Hu, *Small*, 2019, **15**, 1805175.
24 A. Favron, E. Gaufres, F. Fossard, A. L. Phaneuf-L'Heureux, N. Y. Tang, P. L. Levesque, A. Loiseau, R. Leonelli, S. Francoeur, R. Martel, *Nat. Mater.*, 2015, **14**, 826-832.
25 L. Zhang, L.-F. Gao, L. Li, C.-X. Hu, Q.-Q. Yang, Z.-Y. Zhu, R. Peng, Q. Wang, Y. Peng, J. Jin, H.-L. Zhang, *Mater. Chem. Front.*, 2018, **2**, 1700-1706.
26 T. Zhang, Y. Wan, H. Xie, Y. Mu, P. Du, D. Wang, X. Wu, H. Ji, L. Wan, *J. Am. Chem. Soc.*, 2018, **140**, 7561-7567.
27 Y. Liu, P. Gao, T. Zhang, X. Zhu, M. Zhang, M. Chen, P. Du, G.-W. Wang, H. Ji, J. Yang, S. Yang, *Angew. Chem. Int. Ed.*, 2019, **58**, 1479-1483.
28 Y. Cao, B. Zhang, X. Tian, M. Gu, Y. Chen, *Nanoscale*, 2019, **11**, 3527-3533.
29 X. Tang, W. Liang, J. Zhao, Z. Li, M. Qiu, T. Fan, C. S. Luo, Y. Zhou, Y. Li, Z. Guo, D. Fan, H. Zhang, *Small*, 2017, **13**, 1702739.
30 X. Zhu, T. Zhang, D. Jiang, H. Duan, Z. Sun, M. Zhang, H. Jin, R. Guan, Y. Liu, M. Chen, H. Ji, P. Du, W. Yan, S. Wei, Y. Lu, S. Yang, *Nat. Commun.*, 2018, **9**, 4177.
31 C.-X. Hu, Q. Xiao, Y.-Y. Ren, M. Zhao, G.-H. Dun, H.-R. Wu, X.-Y. Li, Q.-Q. Yang, B. Sun, Y. Peng, F. Yan, Q. Wang, H.-L. Zhang, *Adv. Funct. Mater.*, 2018, **28**, 1805311.
32 P. D. Matthews, W. Hirunpinyopas, E. A. Lewis, J. R. Brent, P. D. McNaughter, N. Zeng, A. G. Thomas, P. O'Brien, B. Derby, M. A. Bissett, S. J. Haigh, R. A. W. Dryfe, D. J. Lewis, *Chem. Commun.*, 2018, **54**, 3831-3834.
33 S. Lin, S. Liu, Z. Yang, Y. Li, T. W. Ng, Z. Xu, Q. Bao, J. Hao, C.-S. Lee, C. Surya, F. Yan, S. P. Lau, *Adv. Funct. Mater.*, 2016, **26**, 864-871.
34 B. Zhang, F. Fan, W. Xue, G. Liu, Y. Fu, X. Zhuang, X.-H. Xu, J. Gu, R.-W. Li, Y. Chen, *Nat. Commun.*, 2019, **10**, 736.
35 C.-M. Park, H.-J. Sohn, *Adv. Mater.*, 2007, **19**, 2465-2468.
36 J. Cai, B. Sun, W. Li, X. Gou, Y. Gou, D. Li, F. Hu, *J. Electroanal. Chem.*, 2019, **835**, 1-9.
37 G. Maduraiveeran, M. Sasidharan, V. Ganesan, *Biosens. Bioelectron.*, 2018, **103**, 113-129.
38 R. Kumar, R. G. Pillai, N. Pekas, Y. Wu, R. L. McCreery, *J. Am. Chem. Soc.*, 2012, **134**, 14869-14876.

View Article Online
DOI: 10.1039/D0TC01660H

Anti-Oxidative Passivation and Electrochemical Activation of Black Phosphorus via Covalent Functionalization and Its Nonvolatile Memory Application

Weilin Chen, Shuang Gao,* Zhuolin Xie, Ying Lu, Guodong Gong, Gang Liu,* Jie Shang, Chuang Yao, and Run-Wei Li*

Covalent modification of BP nanosheets with triphenylamine molecules result in better air stability and electrochemical activity, thus enabling potential use for nonvolatile resistive switching memory.